Chapter-4

Spectroscopic studies of Nd^{3+} doped Lead Tungsten Tellurite glasses for the NIR emission at 1062 nm

Paper based on this chapter is published in Optical Materials 39 (2015) 8-15

4.1. Introduction

In recent years, rare earth doped materials are playing a vital role in the modern optical technology as an active constituents to produce low price integrated laser sources, integrated optical amplifiers, 3D display devices, sensors, up-conversion fibres and low loss components [120]. The above mentioned applications possessed by the rare earth doped materials have stimulated the research on rare earth doped glasses [121–125]. Among different rare earth ions, neodymium ion is one of the utmost efficient ions used to prepare solid-state lasers because of its intense emission at 1060 nm [126]. For this reason, trivalent neodymium (Nd^{3+}) ion doped variety of crystals and glasses were studied extensively under 808 and 885 nm laser diode excitation with an aim to develop high power NIR (at 1060 nm) solid state lasers [127,128]. Different glass hosts like borates, phosphates, germanates, vanadates and tellurite families have been studied extensively for this purpose [129-133]. Among all oxide glasses, Lead Tungsten Tellurite (PbF_2-WO_3-TeO_2) glass system (LTT) has unique optical properties.

In the backdrop of the scientific patronages offered by lead fluoride, tungsten oxide and tellurium oxide, in the present work we prepared a germane system namely Lead Tungsten Tellurite (LTT) glass by taking the aforementioned chemicals as constituent elements and doped it with Nd^{3+} ions at different concentrations to study their optical absorption, NIR emission and decay spectral profiles in order to explore the possibility of using these new materials for future photonic devices. Particularly the absorption spectra have been analysed on the basis of Judd-Ofelt (J-O) theory as it is a standard tool in evaluating the radiative properties of the doped rare earth ions in glass hosts. Such measured radiative properties combined with emission spectral data are useful in understand the lasing potentialities of the prepared LTT glasses.

4.2. Experimental

4.2.1. Glass Preparation

The LTT glasses of composition (in mol %) 15 PbF_2 +25 WO_3 + (60-x) TeO_2+ x Nd_2O_3 (here x=0.1, 0.5, 1.0 and 1.5 mol%) were prepared by using melt quenching technique from reagents of analar grade (purity more than 99.9%) in 10 g batches. These glasses are labelled as LTTNd01, LTTNd05, LTTNd10 and LTTNd15 depending on Nd^{3+} ion concentration 0.1, 0.5, 1.0 and 1.5 mol% respectively. Batches containing different concentrations of Nd^{3+} ions in base glass compositions were thoroughly mixed in an agate mortar to get a smooth powder. Such powders were then collected in a silica

crucible and heated in a furnace at 730^{o}C temperature for 30 min. The melt was quenched by pouring onto a circular shaped copper plate and pressed quickly by another plate. The LTT glasses thus prepared were annealed at 400^{o}C for two hours to remove thermal strains and to improve the mechanical strength of the prepared glasses. Finally, the glasses were polished with emery paper before going for experimental measurements.

4.2.2. Physical, absorption, emission and decay spectral measurements

Archimedes principle is used to determine the densities of the Nd^{3+} doped LTT glass samples with water as an immersion liquid. Brewster's angle method with He-Ne laser operating at 632 nm is used to measure the refractive index of the prepared glasses. From the measured density and refractive indices, various other physical properties of the LTT glasses were evaluated using the relevant expressions given in Chapter-2, eq.(2.1-2.11) and are given in Table 4.1.

Absorption spectra for Nd^{3+} doped LTT glasses were recorded at room temperature in the wavelength range 500-900 nm with a spectral resolution of 0.1 nm using a JASCO model V-670 UV-vis-NIR spectrophotometer. The photoluminescence (PL) emission and time-resolved PL measurements were carried out using home-built set ups with 808 nm CW laser as an excitation source. The emission from sample was coupled into a monochromator (Acton SP2300) coupled to CCD (charge coupled detector) through appropriate lenses and filters. For time resolved PL measurements, a frequency generator (5 Hz), lock-in amplifier, digital storage oscilloscope and a monochromator (ANDOR SR-500i-B2) coupled to InGaAs detector through the appropriate lenses and filters are used.

4.3. Results and discussion

4.3.1 Physical properties

The variation of density (g/cm^3), mean atomic volume (g/cm^3/atom), refractive index, average Molecular weight (g), inter Ionic distance (A^o) and field strength(X10^{15} cm^{-2}) as a function of Nd_2O_3 concentration in LTT glasses have been shown in Fig.4.1a. to 4.1c.

Table 4.1.

Various Physical properties of Nd^{3+} ions doped LTT glasses.

Physical properties	**LTTNd01**	**LTTNd05**	**LTTNd10**	**LTTN15**
Density ρ (g cm^{-3})	6.607	6.612	6.619	6.626
Refractive index (n_d)	2.190	2.201	2.213	2.221
Average molecular weight $\bar{M}$(g)	190.6	191.3	192.2	193.1
Nd^{3+}ion concentration N($x10^{21}$ ions/cm^3)	2.086	10.40	20.73	30.98
Mean atomic volume(g/cm^3/atom)	8.870	8.874	8.880	8.884
Dielectric constant (ε)	4.796	4.844	4.897	4.932
Optical dielectric constant (ε-1)	3.796	3.844	3.897	3.932
Reflections losses (R %)	0.139	0.140	0.142	0.143
Molar refraction (R_m) (cm^{-3})	18.89	19.02	19.18	19.31
Polaron radius (Å)	3.150	1.845	1.466	1.283
Inter ionic distance (Å)	7.838	4.588	3.646	3.189
Molecular electronic Polarizability, α ($x10^{-23}cm^3$)	7.500	1.510	0.761	0.511
Field strength ($x10^{15}$ cm^{-2})	3.016	8.804	13.94	18.23
Optical basicity (Λ_{th})	0.464	0.468	0.473	0.477

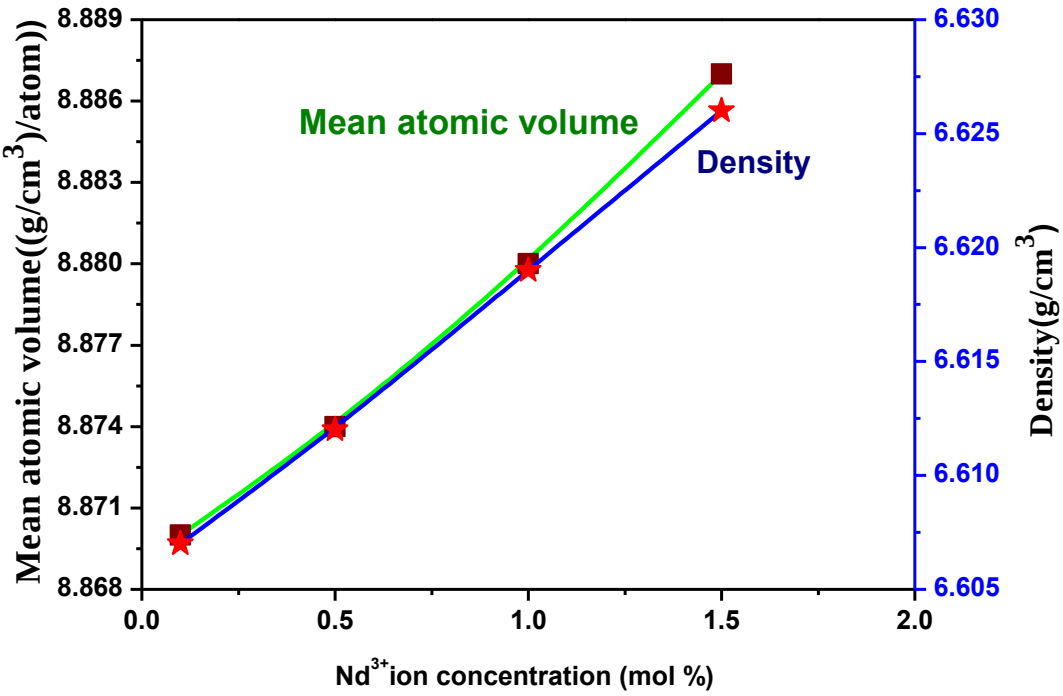

Fig. 4.1(a). The variation of density (g/cm^3) and mean atomic volume (g/cm^3/atom) parameters as a function of Nd^{3+} ion concentration (mol %) in LTT glasses.

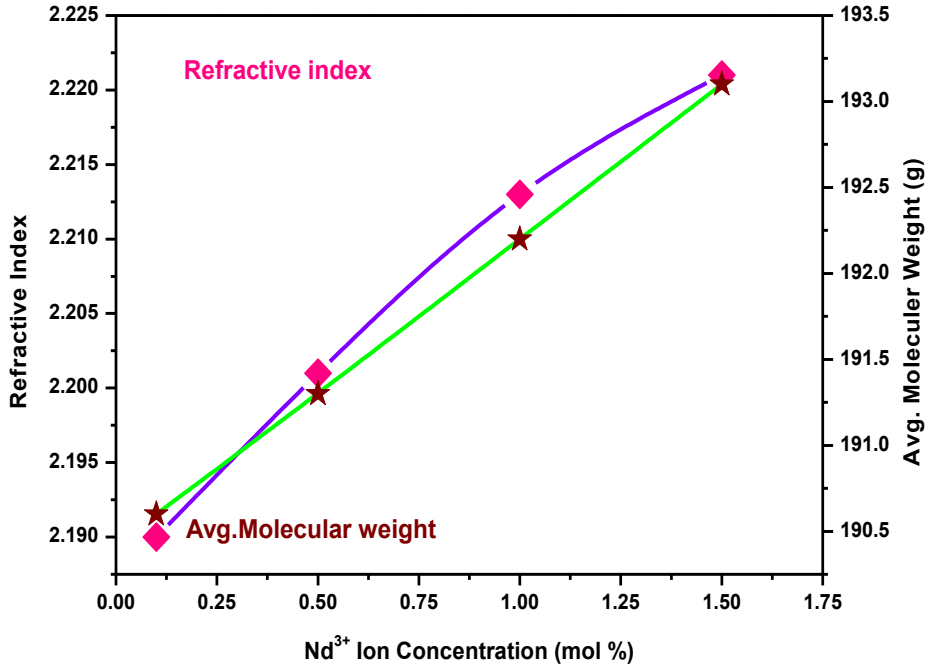

Fig. 4.1(b). The variation of refractive index and average molecular weight (g) parameters as a function of Nd^{3+} ion concentration (mol %) in LTT glasses.

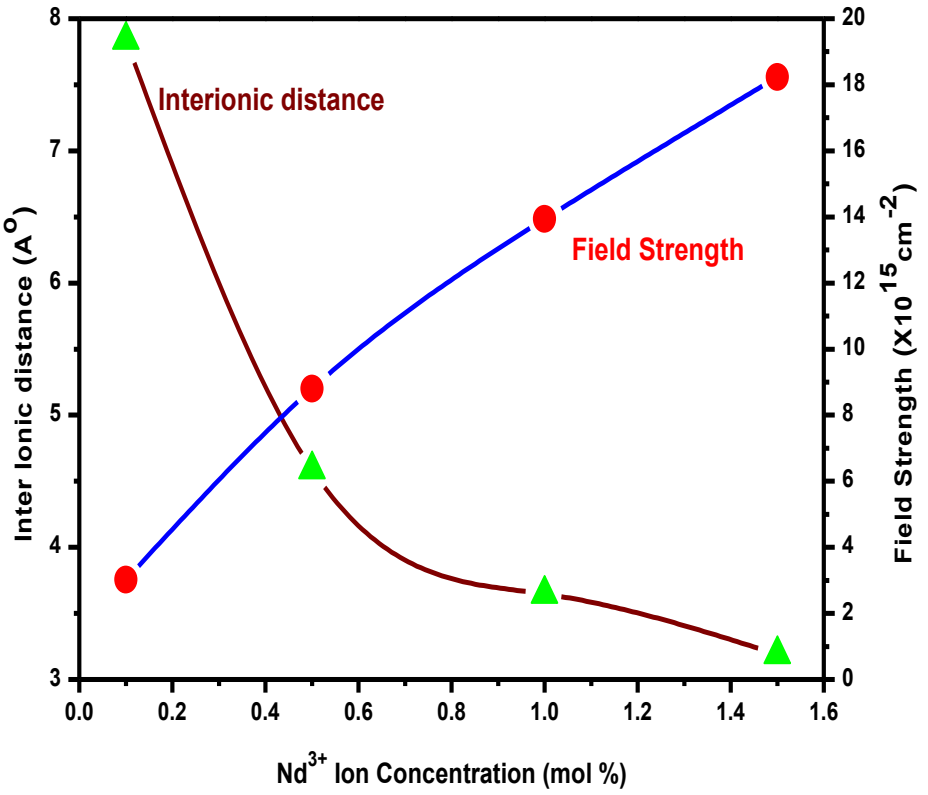

Fig. 4.1(c). The variation of inter ionic distance (A^o) and field strength($X10^{15}$ cm^{-2}) parameters as a function of Nd^{3+} ion concentration (mol %) in LTT glasses.

From Fig.4.1.a it is observed that with increase in Nd^{3+} ion concentration in LTT glasses, the density and mean atomic volume values are also increasing indicating more rigid nature of the prepared LTT glasses. This is further confirmed by increase in average molecular weight and decrease in inter ionic distance values with Nd^{3+} ion concentration as shown in Fig.4.1b & 1c respectively. The tendency of decrease in inter ionic distance in the present glasses indicates that the atoms are more tightly packed as the Nd^{3+} ion concentration increases in these glasses. From Fig.4.1b, it is observed that refractive index of LTT glasses increases with increase in dopant ion concentration. As the density of the LTT glasses are increasing with dopant ion concentration, the denser nature of the glasses relatively increases and will increase the refractive index of the medium with dopant ion concentration. From Fig.4.1c, it can also be seen that the field strength values are increasing with increase in Nd^{3+} ion concentration. This is obvious because, when the rare earth ion concentration in glass increases, the number of ions

available per unit volume will also increase and this will increase the field strength. From Table 4.1, it is also observed that these glasses have molecular electronic polarizability of the order 10^{-23} which is a very low value and hence the present LTT glasses are said to be more stable. In general, the optical basicity of the oxide medium is nothing but the average electron donating power of all oxide atoms present in the medium. For the present system of glasses, the values of optical basicity are increasing with the increase in Nd^{3+} ion concentration. This results in increasing negative charge on the oxygen atom and thus increases covalency in the cation-oxygen bonding.

4.3.2. Optical absorption spectra

Optical absorption spectra for all the LTT glasses doped with Nd^{3+} ions were measured in visible and near infra-red (vis-NIR) regions at room temperature in the wavelength range 500-900 nm. The band positions observed in the absorption spectra of all the glasses is same with minute difference in their intensities.

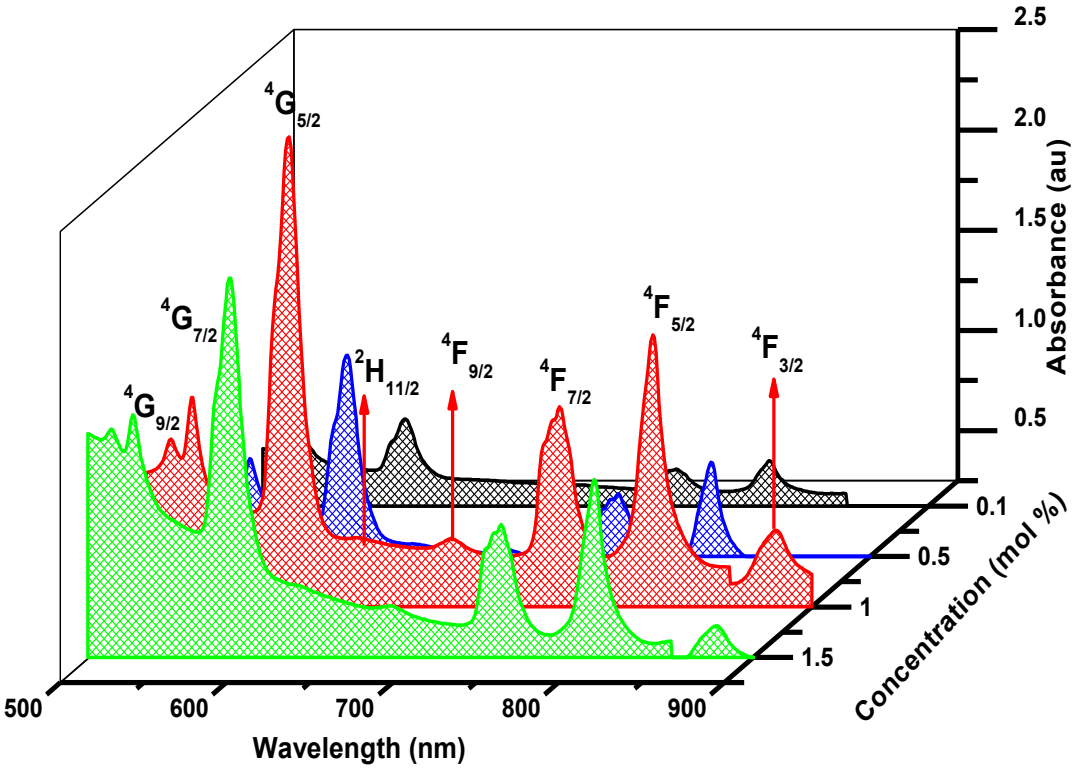

Fig. 4.2. Absorption spectra of Nd^{3+} ions in LTT glasses.

Fig.4.2 shows the optical absorption spectra of Nd^{3+} ions doped LTT glasses in vis-NIR region. As shown in Fig.4.2, the Nd^{3+} ions in all the LTT glasses exhibits eight absorption bands in vis-NIR region at 513, 526, 584, 627, 681, 748, 803 and 877 nm [134,135] corresponding to the transitions $^4I_{9/2} \rightarrow {}^4G_{9/2}$, $^4G_{7/2}$, $^4G_{5/2}$, $^2H_{11/2}$, $^4F_{9/2}$, $^4F_{7/2}$, $^4F_{5/2}$, and $^4F_{3/2}$ respectively [136,105]. Because of the strong absorption of the host glass in UV region, few absorption bands have disappeared in that region. From the identified band positions (cm^{-1}), nephelauxetic ratio ($\bar{\beta}$) and bonding parameters(δ) are evaluated and are given in Table 4.2.

Table 4.2.

Assignment of absorption bands, experimental & calculated oscillator strengths (f_{exp} & f_{cal}) (10^{-6}), rms deviation (δ_{rms}) (10^{-6}), nephelauxetic ratio ($\bar{\beta}$) and bonding parameters (δ) for Nd^{3+} ions doped LTT glasses

Transition	**Wavelength**	**LTTNd01**		**LTTNd05**		**LTTNd10**		**LTTNd15**	
$^4I_{9/2} \rightarrow$	**(nm)**	**f_{exp}**	**f_{cal}**	**f_{exp}**	**f_{cal}**	**f_{exp}**	**f_{cal}**	**f_{exp}**	**f_{cal}**
$^4G_{9/2}$	513	0.975	2.068	2.330	2.776	3.284	3.0521	2.130	2.015
$^4G_{7/2}$	527	4.650	5.064	6.340	6.660	7.610	7.263	5.16	4.732
$^4G_{5/2}$	584	16.83	16.80	27.9	27.881	29.520	29.540	18.100	18.123
$^2H_{11/2}$	627	0.113	0.156	0.510	0.294	0.547	0.328	0.270	0.207
$^4F_{9/2}$	682	0.321	0.524	1.220	1.006	1.959	1.119	0.72	0.721
$^4F_{7/2}$	747	1.426	1.791	4.130	4.206	5.206	4.685	3.530	2.984
$^4F_{5/2}$	803	7.023	6.696	10.63	10.572	11.290	11.738	7.27	7.644
$^4F_{3/2}$	878	3.867	3.857	4.52	4.405	5.08	4.842	3.430	3.246
δ_{rms}		± 0.45		± 0.22		± 0.42		± 0.29	
$\bar{\beta}$		0.9946		0.9948		0.9950		0.9951	
δ		0.537		0.515		0.498		0.488	

The essential mathematical formulae needed for the determination of nephelauxetic ratio and bonding parameter are calculated using eq.(1.3-1.4) are given in chapter-I.` Depending on the field environmental, the bonding parameter (δ) may be positive or

negative indicating covalent or ionic bonding. From Table 4.2, it is observed that the bonding parameter (δ) for all the LTT glasses is found to be positive i.e., the prepared glasses are covalent in nature and the covalent nature decreases gradually with increase in Nd^{3+} ion concentration.

The intensity of absorption bands, which are usually called as oscillator strength (f_{exp}) is directly proportional to the area under the absorption band and can be determined from the absorption spectral features using the relevant equation (1.8) is given in chapter-I. From the absorption spectra, it is noticed that one particular transition namely $^4I_{9/2} \rightarrow {}^4G_{5/2}$ is more intense than other transitions and having large oscillator strengths in all the glasses under investigation. This transition is known as the hypersensitive transition, for which the selection rules $\Delta J \leq 2$; $\Delta L \leq 2$ and $\Delta S = 0$ holds good. The calculated oscillator strengths (f_{cal}) for the f-f transitions of Nd^{3+} ions from its ground state (ψ_J) to the excited state ($\psi'_{J'}$) were determined using J-O theory [47, 48] using equation (1.5). The experimental and calculated oscillator strengths reported in Table 4.2 are in good agreements with each other with less rms deviation. In the process of evaluating J-O parameters (Ω_λ) through a least squares fitting procedure, the necessary reduced matrix elements $\left|\left|U^{\lambda}\right|\right|^2$ were collected from literature [136]. The J-O intensity parameters (Ω_λ) and spectroscopic quality factors of Nd^{3+} doped LTT glasses are given in Table 4.3 along with the reported values [137-151].

J-O intensity parameters are highly useful in explaining the environment around the doped rare earth ions in the host glass. The local structure and bonding nature of rare earth ions can be studied on the basis of magnitudes of the J-O intensity parameters. The bulk properties of the host medium such as rigidity and viscosity of the medium in which the rare earth ions are situated can be explained on the basis of the magnitudes of Ω_4 and Ω_6. From Table 4.3, it is observed that Ω_4 is higher than Ω_6 and Ω_2 and follows the same trend $\Omega_4 > \Omega_6 > \Omega_2$ for all the Nd^{3+} doped LTT glasses. Supplementarily it is perceived that the J-O parameters are increasing from 0.5 to 1 mol% of dopant ion concentration and then decreasing beyond in these glasses. Ideally, the J-O intensity parameters need not show any variation with concentration in the same host owing to the occupation of similar dopant sites.

Table 4.3.

Judd-Ofelt intensity parameters (Ω_λ where λ=2, 4 and 6) (10^{-20} cm^2) for Nd^{3+} ions doped LTT glasses and other reported glasses

Name of the glass	Ω_2	Ω_4	Ω_6	Trend	$\chi=\Omega_4/\Omega_6$	Reference
LTTNd01	1.81	5.27	2.17	$\Omega_4>\Omega_6>\Omega_2$	2.42	Present work
LTTNd05	4.46	5.31	5.14	$\Omega_4>\Omega_6>\Omega_2$	1.03	Present work
LTTNd10	4.54	5.79	5.69	$\Omega_4>\Omega_6>\Omega_2$	1.01	Present work
LTTNd15	2.60	3.91	3.59	$\Omega_4>\Omega_6>\Omega_2$	1.08	Present work
Tellurite	3.80	4.94	4.54	$\Omega_4>\Omega_2>\Omega_6$	1.08	[137]
Germanate	3.09	5.54	4.48	$\Omega_4>\Omega_6>\Omega_2$	1.23	[137]
LBNNd10with HST	4.81	5.55	3.73	$\Omega_4>\Omega_2>\Omega_6$	1.48	[138]
NaTFP	3.01	5.26	4.21	$\Omega_4>\Omega_6>\Omega_2$	1.25	[139]
Nbl	3.12	4.84	3.28	$\Omega_4>\Omega_6>\Omega_2$	1.03	[139]
LaF_3	0.35	2.57	2.50	$\Omega_4>\Omega_6>\Omega_2$	1.03	[139]
Tellurite	3.62	4.21	2.95	$\Omega_4>\Omega_6>\Omega_2$	1.43	[140]
Germanate	3.09	5.54	4.80	$\Omega_4>\Omega_6>\Omega_2$	1.15	[141]
CaNb Glass	4.40	5.20	2.70	$\Omega_6>\Omega_4>\Omega_2$	1.92	[142]
LBTAFNd05	5.82	1.88	4.76	$\Omega_2>\Omega_6>\Omega_4$	0.39	[143]
ZBLAN	5.09	3.12	7.16	$\Omega_2>\Omega_6>\Omega_4$	0.43	[144]
SPB1	4.81	1.97	3.94	$\Omega_2>\Omega_6>\Omega_4$	0.50	[145]
LBT	1.05	1.50	4.20	$\Omega_6>\Omega_4>\Omega_2$	0.35	[146]
30 B_2O_3-70PbO	3.52	2.98	5.48	$\Omega_6>\Omega_2>\Omega_4$	0.54	[147]
Flouride	1.95	3.65	4.17	$\Omega_6>\Omega_4>\Omega_2$	0.87	[148]
Silicate	4.71	4.54	5.05	$\Omega_6>\Omega_2>\Omega_4$	0.89	[149]
Phosphate	6.30	4.00	4.30	$\Omega_2>\Omega_6>\Omega_4$	0.93	[150]
$TeO_2WO_3PbONd_2O_3$	4.88	4.05	3.82	$\Omega_2>\Omega_4>\Omega_6$	1.06	[151]

But, in the present work, the observed variation in J-O intensity parameters may be attributed to the tendency of clustering of dopant ions. Also, increasing concentration may produce site-to-site variation and subsequently the local crystal field as well as the asymmetry around the dopant ions may change and may cause variations in J-O parameters. The J-O intensity parameter Ω_2 increases from glass LTTNd01 to LTTNd10 and then decreases for LTTNd15. The intensity of hypersensitive transition

and Ω_2 are high for LTTNd10 glass indicating that it has the highest covalence and asymmetry around Nd^{3+} ions.

4.3.3. Photoluminescence spectra and radiative properties

The NIR photoluminescence spectra of LTT glasses doped with Nd^{3+} ions when excited under 808 nm CW laser source is shown in Fig. 4.3.

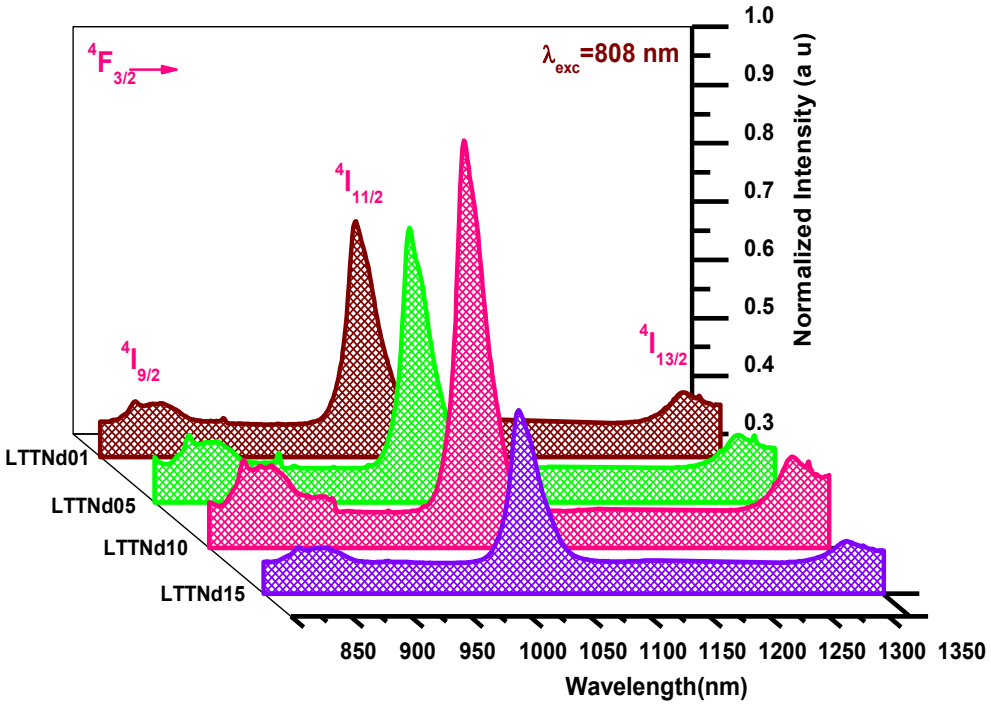

Fig. 4.3. Emission spectra Nd^{3+} ions in LTT glasses

The Nd^{3+} ions excited to $^4F_{5/2}$ level in LTT glasses are immediately falling to $^4F_{3/2}$ metastable state through fast non-radiative relaxation as indicated in Fig. 4.4.

The resultant PL spectra shown in Fig.4.3 consist of three emission bands at 878, 1062 and 1339 nm corresponding to the transitions $^4F_{3/2}\rightarrow{}^4I_{9/2}$, $^4F_{3/2}\rightarrow{}^4I_{11/2}$ and $^4F_{3/2}\rightarrow{}^4I_{13/2}$ respectively. From the PL spectra, it is observed that, the intensity of all the emission transitions increases with increase in Nd^{3+} ion concentration up to 1.0 mol% and then decreasing beyond showing concentration quenching, which can be attributed to the interaction between the excited Nd^{3+} ions and energy transfer observed between Nd^{3+} ions. Among all the emission transitions, a transition $^4F_{3/2}\rightarrow{}^4I_{11/2}$ observed at 1062 nm has highest intensity for LTTNd10 glass. The absorption, excitation and emission mechanisms are shown in Fig.4.4 along with the possible cross-relaxation channel.

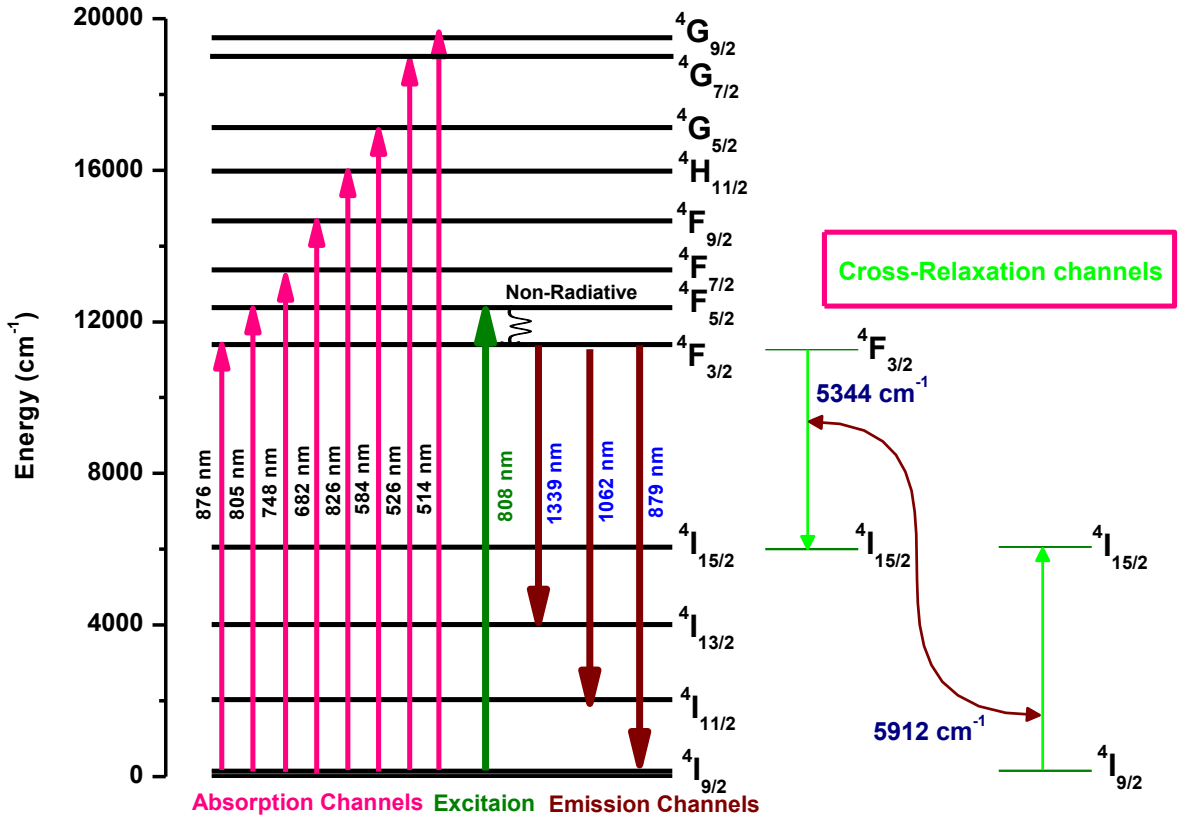

Fig. 4.4. Schematic energy level scheme of Nd^{3+} ions in LTTNd10 glass along with the absorption, excitation, emission and cross-relaxation channels

The J-O intensity parameters are coupled with the emission spectral data, to evaluate different radiative properties such as radiative transition probability (A_R), total transition probability (A_T), branching ratios (β_R) and radiative lifetimes (τ_R) using the relevant equations (1.10-1.13) are given in chapter-I. In general, the stimulated emission cross-section is independent on the J-O parameters and half band widths ($\Delta\lambda_{eff}$) of the emission bands, which are effected by host glass composition. In addition, the intensity of $^4F_{3/2} \rightarrow {}^4I_{11/2}$ laser transitions at 1062 nm depends only on the Ω_4 and Ω_6 parameters because of triangle rule $|J' - J| \leq \lambda \leq |J' + J|$ [144]. The A_R, A_T and τ_R values observed for all the emission transitions of Nd^{3+} ions in LTT glasses are given in Table 4.4.

Table 4.4.
Radiative transition probabilities (A_R) (s^{-1}), total transition probabilities (A_T) (s^{-1}), experimental & radiative branching ratios (β_{exp} & β_R) and radiative lifetimes (τ_R) (μs) for the emission transitions of Nd^{3+} ions doped LTT glasses.

Transition $^4F_{3/2}$	Spectral parameters	LTTNd01	LTTNd05	LTTNd10	LTTNd15
$^4I_{9/2}$	A_R	4020.12	4663.76	5148.49	3467.25
	A_T	7342.46	10866.82	12040.22	7926.80
	β_{exp}	0.226	0.327	0.200	0.220
	β_R	0.547	0.429	0.427	0.437
	τ_R	136	92	83	126
$^4I_{11/2}$	A_R	2896.56	5169.21	5742.55	3727.74
	A_T	7342.46	10866.82	12040.22	7926.80
	β_{exp}	0.701	0.606	0.709	0.687
	β_R	0.394	0.475	0.476	0.470
	τ_R	136	92	83	126
$^4I_{13/2}$	A_R	405.68	984.97	1095.14	697.46
	A_T	7342.46	10866.82	12040.22	7926.80
	β_{exp}	0.072	0.066	0.095	0.091
	β_R	0.055	0.090	0.091	0.088
	τ_R	136	92	83	126

These values are useful to determine how fast an excited level gets depopulated. The radiative branching ratios (β_R) used to calculate the relative intensities of all the luminescence transitions originating from an excited state are given in Table 4.4 along with experimental branching ratios. The experimental branching ratios (β_{exp}) can be determined from the relative areas of the emission transitions. From Table 4.4, it can be seen that the experimental branching ratios are higher than radiative branching ratios for all the LTT glasses. The highest value of branching ratio (β_R) is an attractive feature for low threshold and high gain applications of lasers. From Table 4.4, it can be observed that, the LTTNd10 glass has highest branching ratio for the transition $^4F_{3/2} \rightarrow {}^4I_{11/2}$ and can be recommended as an efficient lasing transition. The stimulated

emission cross-section (σ_{se}) for all the luminescence transitions have been calculated using eq.(1.14) given in chapter-I and are tabulated in Table 4.5.

Table 4.5.
Emission peak wavelength (λ_P) (nm), effective band widths($\Delta\lambda_P$) (nm),stimulated emission cross-sections (σ_{se}) ($x10^{-19}$) (cm^2), gain band width(σ_{se} x $\Delta\lambda_p$) (10^{-26}) (cm^3) and optical gain parameters (σ_{se} x τ_R) (10^{-23}) (cm^2 s) for the emission transitions of Nd^{3+} ions doped LTT glasses

Transition $^4F_{3/2}$	Spectral parameters	LTTNd01	LTTNd05	LTTNd10	LTTNd15
$^4I_{9/2}$	λ_p	878	878	878	878
	$\Delta\lambda_p$	5.56	5.28	4.72	5
	σ_{se}	1.19	1.44	1.76	1.17
	σ_{se} x $\Delta\lambda_p$	6.61	7.59	8.29	5.83
	σ_{se} x τ_R	1.62	1.32	1.46	1.47
$^4I_{11/2}$	λ_p	1062	1062	1062	1062
	$\Delta\lambda_p$	6.94	5.55	4.16	5.55
	σ_{se}	1.47	3.24	4.75	2.30
	σ_{se} x $\Delta\lambda_p$	10.23	18.01	19.80	12.80
	σ_{se} x τ_R	2.00	2.98	3.94	2.89
$^4I_{13/2}$	λ_p	1339	1339	1339	1339
	$\Delta\lambda_p$	3.75	3.33	3.19	3.611
	σ_{se}	0.96	2.60	2.99	1.67
	σ_{se} x $\Delta\lambda_p$	3.61	8.67	9.54	6.03
	σ_{se} x τ_R	1.31	2.39	2.48	2.10

The stimulated emission cross-section which influences the potential laser performance signifies the energy extraction from the lasing material. From Table 4.5, it is observed that LTTNd10 glass possess highest stimulated emission cross-section than the other glasses for the transition $^4F_{3/2}\rightarrow{}^4I_{11/2}$ at 1062 nm. In order to understand optical amplification performance of the LTT glasses, we have evaluated gain band width (σ_{se} x $\Delta\lambda_P$) and optical gain parameters (σ_{se} x τ_R) and are given in Table 4.5. From Table 4.5, it is observed that, among all the LTT glasses studied here, the LTTNd10 glass possesses highest values of optical gain parameters and gain band width for $^4F_{3/2}\rightarrow{}^4I_{11/2}$

transition and hence can be suggested for optical amplification also. Hence in the present system of LTT glasses, the LTTNd10 glass can be recommended as a suitable host for lasing emission at 1062 nm and also for optical amplification.

4.3.4. Decay Curve Analysis

The decay curves recorded for the luminescence from $^4F_{3/2}$ level of Nd^{3+} ion in LTT glasses are shown in Fig. 4.5.

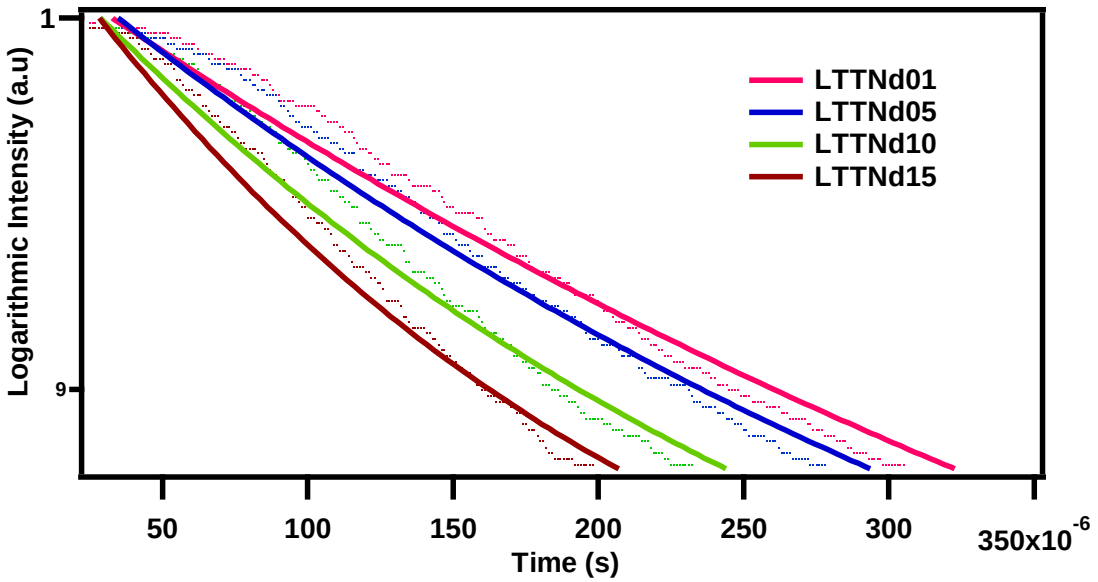

Fig. 4.5. Emission decay profiles for $^4F_{3/2} \rightarrow {}^4I_{11/2}$ transition of Nd^{3+} ions in LTT glasses. Solid lines are from exponential curve fits.

From Fig. 4.5, it can be observed that the decay profiles for all the LTT glasses are single exponential in nature irrespective of Nd^{3+} ion concentration. This may be due to fast decay of Nd^{3+} ions (or) negligible effect of ligands on Nd^{3+} ions. From the decay curves, the experimental lifetimes (τ_{exp}) are evaluated by using the relevant expression given in literature [152] and are given in Table 4.6 along with the radiative lifetimes (τ_R).

Table 4.6.

Radiative and experimental lifetimes (τ_R & τ_{exp}) (μs), quantum efficiency (η) and multi-phonon relaxation rate (W_{NR}) (μs^{-1}) for $^4F_{3/2} \rightarrow {}^4I_{11/2}$ emission transition of Nd^{3+} ions doped LTT glasses.

Name of the Sample	τ_R	τ_{exp}	η (%)	W_{NR}
LTTNd01	136	91	67	3636
LTTNd05	92	73	79	2829
LTTNd10	83	68	82	2657
LTTNd15	126	61	48	8456

From Table 4.6, it can be observed that the experimental lifetimes were found to be decreasing with increasing in Nd^{3+} ion concentration in LTT glasses. The quantum efficiency, an another important parameter used to understand the lasing efficiency of a host material is defined as the ratio between emitted light intensity and absorbed pump intensity and is evaluated using the expression in given in our previous paper [152]. Such quantum efficiency values along with radiative and measured lifetimes are given in Table 4.6. From Table 4.6, it is observed that, among all the LTT glasses, LTTNd10 glass possess highest quantum efficiency for the transition $^4F_{3/2} \rightarrow {}^4I_{11/2}$ (1062 nm). The experimental lifetimes for LTT are found to be less than the radiative lifetimes. The relaxation from excited state is represented by both radiative and non-radiative decay modes. The non-radiative decay rate WNR for all the LTT glasses was estimated using the equation (1.15) given in chapter-I.

The radiative decay rate is affected by the local crystal-field symmetry around the Nd^{3+} ion and to some extent due to local vibration density of the states of the host. The non-radiative decay rate is due to multi-phonon relaxation process. The prominent processes contributing to the reduction of radiative decay should be considered in order to explain the mechanism of non-radiative process. This non-radiative process (W_{NR}) is undesirable for amplifying devices as they need population inversion. In the present work, the quantum efficiency of the $^4F_{3/2} \rightarrow {}^4I_{11/2}$ transition increases up to 1 mol% of Nd^{3+} ion concentration and then decreases. The non-radiative relaxation rates measured for the LTT glasses are given in Table 4.6. From Table 4.6, it is observed that, among all the LTT glasses, the LTTNd10 glass possess lowest non-radiative relaxation rate

and highest quantum efficiency. Hence the LTTNd10 glass is aptly suitable for NIR laser emission at 1062 nm. Table 4.7 gives the comparison of experimental branching ratios, stimulated emission cross-section and quantum efficiency for LTTNd10 glass with commercial systems and other hosts [134, 138-140, 151, 153-159]. Among all the LTT glasses LTTNd10 glass possess better values of branching ratios, stimulated emission cross-section and quantum efficiency than the other reported glass systems. Hence LTTNd10 glass can be recommended as suitable host to produce efficient lasing action in NIR region at 1062 nm.

Table 4.7.

Comparison of branching ratio (β_R), stimulated emission cross-section (σ_{se} X 10^{-22} cm^2) and quantum efficiency (η (%)) of LTTNd10 glass for $^4F_{3/2} \rightarrow {}^4I_{11/2}$ emission transition with commercial glass systems and other Nd^{3+} doped glass hosts

Name of the Glass system	β_{exp}	σ_{se}	η (%)	References
Commercial Glass Systems				
LTTNd10	0.709	4.75	82	Present work
LHG-80	-	4.2	-	[153, 154]
LG-770	-	3.9	-	[153, 154]
Q-88	-	4.0	-	[153, 154]
LHG-8	-	3.7	-	[153, 154]
LG-750	-	3.6	-	[138,155]
Other Glass Systems				
BNa4	0.52	4.94	-	[134]
NaTFP	0.735	3.89	71	[139]
LiTFP	0.764	3.75	62	[139]
KTFP	0.734	4.50	68	[139]
TZNLN	0.77	4.28	-	[140]
LBTAFNd05	0.62	2.60	23	[143]
$TeO_2WO_3PbONd_2O_3$	0.45	-	-	[151]
PKMAFN	0.51	4.40	-	[153]
MgTP	0.73	3.82	72	[156]
CaTP	0.73	3.95	75	[156]
SrTP	0.73	4.03	84	[156]
NdF_3 based glass	-	4.68	-	[157]
CLiBT	0.52	3.90	-	[158]
SFB	0.50	3.46	-	[159]

4.4. Conclusion

Lead Tungsten Tellurite (LTT) glasses doped with different concentration of Nd^{3+} ions were prepared by employing melt quenching method and characterized by using the spectroscopic techniques such as optical absorption, emission and decay spectral measurements to optimise the concentration of the doped rare earth ions for better luminescence efficiency. From the measured branching ratios, emission cross-sections and quantum efficiency, it is concluded that the LTT glasses are better suited for NIR laser emission applications. The gain band width (σ_{se} x $\Delta\lambda_p$) (10^{-26}) (cm^3) and optical gain parameters (σ_{se} x τ_R) (10^{-23}) (cm^2 s) measured for LTT glasses suggests the suitability of these devices for optical amplification applications. Among all the LTT glasses studied here, the LTTNd10 glass possessing better lasing potentialities and optical amplification with more branching ratio, emission cross-section, quantum efficiency, optical gain and gain band width values. Based on the luminescence characteristic parameters measured for all the LTT glasses, it is suggested that LTTNd10 glass is aptly suitable for optical amplification as well as for efficient NIR emission at 1062 nm.